

Impaired Visual Cortical Plasticity in Schizophrenia

Idil Çavuş, Robert M.G. Reinhart, Brian J. Roach, Ralitza Gueorguieva, Timothy J. Teyler, Wesley C. Clapp, Judith M. Ford, John H. Krystal, and Daniel H. Mathalon

Background: Impaired cortical plasticity may be part of the core pathophysiology of schizophrenia (SZ). Long-term potentiation is a form of neuroplasticity that has been recently demonstrated in humans by showing that repetitive visual stimulation produces lasting enhancement of visual evoked potentials (VEP). Using this paradigm, we examined whether visual cortical plasticity is impaired in SZ.

Methods: Electroencephalographic data were recorded from 19 SZ and 22 healthy control (HC) subjects during a visual long-term potentiation paradigm. Visual evoked potentials were elicited by standard visual stimuli (~.83 Hz, 2-minute blocks) at baseline and at 2, 4, and 20 minutes following exposure to visual high-frequency stimulation (HFS) (~8.8 Hz, 2 minutes) designed to induce VEP potentiation. To ensure attentiveness during VEP assessments, subjects responded with a button press to infrequent (10%) target stimuli. Visual evoked potentials were subjected to principal components analysis. Two negative-voltage components prominent over occipital-parietal electrode sites were evident at 92 msec (C1) and at 146 msec (N1b). Changes in C1 and N1b component scores from baseline to the post-HFS assessments were compared between groups.

Results: High-frequency stimulation produced sustained potentiation of visual C1 and N1b in HCs but not in SZs. The HCs and SZs had comparable HFS-driven electroencephalographic visual steady state responses. However, greater visual steady state responses to the HFS predicted greater N1b potentiation in HCs but not in SZs. Schizophrenia patients with greater N1b potentiation decreased their reaction times to target stimuli.

Conclusions: Visual cortical plasticity is impaired in schizophrenia, consistent with hypothesized deficits in *N*-methyl-D-aspartate receptor function.

Key Words: Evoked potential, long-term potentiation, plasticity, schizophrenia, visual cortex

Impaired neuroplasticity may underlie psychotic symptoms and cognitive deficits in schizophrenia (SZ) (1,2). Several SZ risk genes are implicated in the regulation of synaptic plasticity (3,4), and their expression in animal models results in *N*-methyl-D-aspartate (NMDA) receptor hypofunction and impaired long-term potentiation (LTP) (5–7). Activation of NMDA receptors is critical for the induction of LTP, a form of experience-dependent synaptic plasticity and a leading cellular mechanism for learning and memory (8). NMDA receptor blockade in healthy people can induce SZ-like psychotic symptoms and cognitive impairments (9,10), consistent with the hypothesis that deficient synaptic plasticity contributes to SZ symptomatology.

Until recently, direct evidence for impaired LTP in SZ has been lacking. To date, two methods for noninvasive evaluation of cortical plasticity in humans have been developed; one uses transcranial magnetic stimulation to probe motor cortex, and another uses patterned visual or auditory stimulation and electroencephalogram (EEG) to evaluate sensory cortex (8,11). A transcranial mag-

netic stimulation paired associative stimulation study demonstrated that motor evoked potential facilitation, which was associated with enhanced motor skill learning, was impaired in SZ (12,13).

Clapp *et al.* (11) and Teyler *et al.* (14) developed an EEG-based method to measure sensory-induced cortical potentiation in humans. This method closely approximates the typical LTP paradigm in animal models, which uses electrical high-frequency stimulation (HFS) to tetanize afferent pathways, rapidly inducing a persistent increase in the postsynaptic response. In anesthetized or awake rodents, visual LTP can be induced not only by electrical HFS (15) but also by visual HFS (16) or daily visual stimulation (17–19), wherein visual stimulation induces repetitive synchronous afferent activity and expression of LTP in thalamocortical synapses of visual cortex. Further, this form of sensory potentiation has the hallmarks of synaptic LTP, including duration, input specificity, mutual occlusion with electrically induced LTP, NMDA-receptor dependency, postsynaptic α -amino-3-hydroxy-5-methyl-4-isoxazolepropionic acid (AMPA) receptor insertion, and requirement for protein kinase M ζ activation, a kinase known to maintain LTP and memory (16–19). As such, it is thought to represent an endogenous form of naturally occurring sensory LTP (17,19). Similarly, in humans, visual HFS with a checkerboard (i.e., photic tetanus) produces lasting enhancement of a visual evoked potential (VEP) component recorded from occipital scalp electrodes (14). This visual plasticity also has characteristics of synaptic LTP, including persistence, input specificity, frequency-dependence, and depotentiation (11,14,20–22).

Interestingly, the visual HFS used to induce VEP potentiation in humans (11,14) is similar to the visual stimulation used to drive visual steady state responses (VSSR) (23,24), wherein EEG power and phase synchrony are enhanced at the driving frequency. Visual steady state response reductions in SZ (25) have been reported for high alpha (>10 Hz) and beta (26) stimulation rates using low-luminance, low-spatial frequency stimuli (27,28). Importantly, VSSR is modulated by attention in both healthy control subjects (HC) and SZ patients (25,29,30). To date, the relationship between VSSR EEG

From the Department of Psychiatry (IC, RMGR, RG, JMF, JHK, DHM), Yale University, New Haven, Connecticut; Department of Psychiatry (BJR, JMF, DHM), University of California; San Francisco Veterans Affairs Medical Center (BJR, JMF, DHM), San Francisco, California; School of Public Health and School of Medicine (RG), Yale University, New Haven, Connecticut; Washington-Wyoming-Alaska-Montana-Idaho Regional Medical Education Program (TT), University of Idaho, Moscow, Idaho; NeuroScouting LLC (WCC), Cambridge, Massachusetts; Schizophrenia Biological Research Center (JHK), Veterans Affairs Connecticut Healthcare System; and Abraham Ribicoff Research Facilities (JHK), Connecticut Mental Health Center, New Haven, Connecticut.

Address correspondence to Daniel H. Mathalon, Ph.D., M.D., Mental Health Service 116D, San Francisco Veterans Affairs Medical Center, 4150 Clement Street, San Francisco, CA 94121; E-mail: daniel.mathalon@ucsf.edu.

Received Jun 10, 2011; revised Dec 17, 2011; accepted Jan 10, 2012.

Table 1. Subject Demographics and Clinical Characteristics

| | Healthy Subjects (n = 22) Mean (SD) | Schizophrenia Patients (n = 19) Mean (SD) | p Value |
|---|---|---|---------|
| Age (Years) | 37.8 (13.3) | 40.0 (13.5) | .6059 |
| Gender | | | |
| Male | 17 | 16 | |
| Female | 5 | 3 | |
| Education (Years) | 16.1 (3.0) | 13.0 (1.5) | .0002 |
| Parental SES ^a | 34.9 (14.8) | 37.3 (16.5) | .6277 |
| Illness Duration (Years) | — | 16.3 (11.6) Range 1–39 | |
| PANSS Score | | | |
| Total | | 57.1 (9.9) | |
| Negative | | 14.8 (8.5) | |
| Positive | | 13.7 (8.2) | |
| General psychopathology | | 28.7 (14.9) | |
| Antipsychotic Dosage ^b (Chlorpromazine Equivalents) | | 421.5 (426.6) mg Range 50–1600 mg | |

PANSS, Positive and Negative Syndrome Scale; SD, standard deviation; SES, socioeconomic status.

^aHollingshead Scale of Socioeconomic Status; smaller scores indicate higher parental SES.

^bAll patients except one were treated with atypical antipsychotics.

power driven by HFS and subsequent VEP potentiation has not been examined.

Schizophrenia is associated with visual learning and memory deficits (31–34), as well as early visual processing impairments that contribute to deficits in higher order visual processing and overall functioning (35–40). Given the putative role of NMDA receptor hypofunction in mediating these and other SZ deficits, we used a visual HFS paradigm previously shown to potentiate VEPs (14) to test the hypotheses that 1) visual plasticity is deficient in SZ; 2) SZ patients have a normal VSSR to tetanizing HFS, indicating that their deficient potentiation is not due to reduced attention to the tetanus; and 3) the VSSR to HFS, reflecting oscillatory entrainment of visual cortical neurons, is directly related to the magnitude of visual potentiation.

Methods and Materials

Subjects

All subjects provided written informed consent (Table 1). Schizophrenia patients (n = 19) were recruited from local clinics and met criteria for schizophrenia based on a Structured Clinical Interview for DSM-IV (41). Symptoms were rated within 2 weeks of EEG recording using the Positive and Negative Syndrome Scale (PANSS) (42). Healthy control subjects (n = 22) were recruited from the local community and had no history of major DSM-IV Axis I

disorders (based on Structured Clinical Interview for DSM-IV) and no first-degree relatives with SZ or bipolar disorder (43).

Other exclusion criteria were benzodiazepine use, alcohol or substance abuse 30 days before enrollment, history of alcohol or substance dependence (except nicotine), neurological or medical illness compromising the central nervous system, head injury with loss of consciousness, and left-handedness based on a quantitative scale (44). All subjects had normal or corrected-to-normal vision. The groups were matched on age and parental socioeconomic status (45) but not education. The study was approved by the Institutional Review Boards of the West Haven Veterans Affairs and Yale University.

Experimental Paradigm

The paradigm (modified from [14]) involved assessment of VEPs before and after exposure to tetanizing visual HFS. While maintaining focus on a central fixation cross, subjects viewed visual stimuli presented centrally against a white background on a 15-inch liquid crystal display color monitor (800 × 600 pixels; 60 Hz refresh rate) located 57 cm in front of them.

Visual Evoked Potential Assessments. Each 2-minute VEP assessment block comprised a pseudorandom oddball sequence of 90% standard and 10% target stimuli (duration 33 msec; Figure 1A) (14) presented at ~83 Hz (1216 msec mean stimulus-onset asynchrony, range 1075–1340 msec), selected to be below the 1 Hz rate

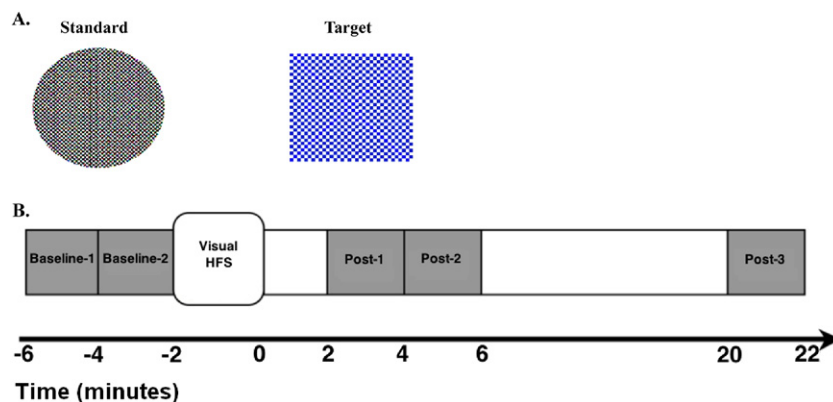


Figure 1. (A) Visual stimuli used in the paradigm. Left: standard circle black and white checkerboard stimulus (8 cm diameter, subtending 8° of visual angle, each check subtending .3°) presented during visual high-frequency stimulation (HFS) and visual evoked potential (VEP) assessment blocks. Right: target square blue and white checkerboard stimulus (9 × 9 cm, subtending 9° of visual angle, each check subtending .5°) presented infrequently during VEP assessment blocks. (B) Timeline of the visual potentiation paradigm. An unrelated auditory task was performed in the intervals between VEP assessment blocks. Baseline-1, 4 to 6 minutes before HFS; Baseline-2, 2 to 4 minutes before HFS; Post-1, 2 to 4 minutes after HFS; Post-2, 4 to 6 minutes after HFS; Post-3, 20 to 22 minutes after HFS.

previously shown to cause VEP depotentiation (14). Visual evoked potentials were elicited by a standard circle (black and white checkerboard). To focus and monitor attention, subjects responded to a target square (blue and white checkerboard) with a right-handed button press, equally emphasizing speed and accuracy. VEP assessment blocks were administered 4 minutes (baseline-1) and 2 minutes (baseline-2) before HFS and 2 minutes (post-1), 4 minutes (post-2), and 20 minutes (post-3) after HFS (Figure 1B). An unrelated auditory task was performed in the intervals between successive post-HFS VEP blocks.

High-Frequency Stimulation. The 2-minute HFS block designed to induce potentiation comprised repeated presentation of the standard circle at ~8.87 Hz (113 msec mean stimulus-onset asynchrony, range 99–116 msec), a rapid flicker rate below the perceptual fusion threshold (14).

EEG Methods

EEG Acquisition. During the paradigm, EEG was recorded from subjects seated in an electrically and acoustically shielded booth using a 32-channel Neuroscan Synamps amplifier (Compumedics, Charlotte, North Carolina). Data were acquired continuously (.05–200 Hz bandpass filter, 1000 Hz digitization rate) from 29 silver/silver chloride sintered electrodes (Easycap, Munich, Germany) in an extended 10-20 system montage (Figure 2) with a linked mastoid reference and a forehead (FPz) ground. Electro-oculograms were recorded horizontally (horizontal electro-oculogram [HEOG]) from the outer canthi of the eyes and vertically (vertical electro-oculogram [VEOG]) from above and below the right orbit. Electrode impedances did not exceed 10 k Ω .

EEG Processing. Electroencephalogram data were analyzed using Brain Vision Analyzer (Brain Products, Munich, Germany) and custom MATLAB (MathWorks, Natick, Massachusetts) scripts. Continuous data were digitally low-pass filtered at 50 Hz (48 dB/octave) and 600 msec (–100 to 500 msec) epochs were extracted, time-locked to the standard circle onsets. After ocular correction using VEOG/HEOG data (46), epochs were re-referenced to Fz, baseline-corrected using the 100-msec prestimulus baseline, and truncated at 250 msec. Epochs containing VEOG or HEOG activity exceeding $\pm 50 \mu\text{V}$ or EEG artifacts exceeding $\pm 70 \mu\text{V}$ were excluded. The number of trials after artifact rejection did not significantly differ between groups. Epochs were averaged, generating VEPs for baseline and post-HFS assessments.

Principal Components Analysis. A temporal principal components analysis (PCA), implemented in MATLAB (47–51), was conducted to extract VEP components that appeared to show post-HFS potentiation in the grand average VEP overlays. Visual evoked potential waveforms (amplitudes at each of the 350-msec time points) from all electrodes ($n = 29$), all assessments (two baseline and three post-HFS), and all subjects ($n = 41$) were submitted to a covariance matrix PCA. All components were retained and subjected to promax rotation, yielding oblique temporal factors corresponding to major VEP components (47,49,51). Factor scores for selected components were saved for subsequent analyses.

HFS-Driven Visual Steady State Response. Electroencephalogram data recorded during HFS were spectrally decomposed using a Fast Fourier Transform. First, a 1-Hz high-pass filter was applied to remove slow drifts. Second, a 120-second Hanning window was applied to minimize frequency leakage (52). Third, the Fast Fourier Transform was applied, yielding a power spectrum. Power values in the frequency bin closest to the HFS frequency (~8.87 Hz), representing the VSSR to HFS, were extracted for subsequent analyses.

Statistical Analyses

Mean Comparisons. Effects of group (HC, SZ), time (baseline, post-1, post-2, post-3), and sometimes electrode site on VEP factor scores were analyzed with mixed effects models (53) using SAS PROC MIXED software (SAS Institute Inc., Cary, North Carolina). For all models, the best-fitting variance-covariance structure was selected based on Schwarz Bayesian information criterion, and then backward elimination was performed on factors affecting the mean. The group \times time interaction was of primary interest in all models. Post hoc comparisons within and between groups were conducted to parse significant interactions. Mixed effects models were also used to compare groups on accuracy and reaction times associated with responses to target stimuli presented during VEP assessments. Visual steady state responses were compared between groups using a *t* test. For all effects tested, $\alpha = .05$.

Correlations. General linear models examined associations among VEP factor change scores (i.e., potentiation score, defined as post-3 minus baseline), as well as their associations with HFS-driven VSSRs and target reaction time change scores (post-3–baseline). The models included the predictor variable, group, and their interaction, with the interaction testing whether regression line slopes differed between the groups. Pearson correlations between VEP factor change scores and PANSS Positive and Negative subscale scores were examined in SZ patients. Tests were Bonferroni corrected using a familywise α of .05 within each domain of measures.

Results

VEP Component Potentiation

Grand average VEPs for baseline and each post-HFS assessment in HCs and SZs are presented in Figure 2. In HCs, HFS appeared to potentiate two VEP components. The first, referred to as C1 (54) (also called N1 [14]), is a prominent negative component between 100 and 120 msec that is maximal at occipital midline sites and flattens out or reverses polarity laterally. The second, referred to as N1b (14), is another negative component peaking at 150 msec that is prominent at lateral parieto-occipital sites. In HCs (Figure 2A), the amplitudes of both components increased (i.e., enhanced negativity) following HFS. For C1, the increase was most evident at Oz. For N1b, the increase was prominent at lateral parieto-occipital sites but also evident at midline sites (Oz, POz). In SZ, the components were evident in the baseline VEPs but did not appear to potentiate following HFS (Figure 2B).

PCA Results

Inspection of the VEP PCA factor loadings (Figure 3) reveals two factors peaking at 92 msec and 146 msec corresponding to the C1 and N1b VEP components and accounting for 13% and 9.7% of the variance, respectively. Furthermore, scalp topographies of these PCA factors (Figures 4 and 5) are consistent with C1 and N1b scalp distributions (Figure 2). Accordingly, the factor scores corresponding to the C1 and N1b components were extracted for all electrodes and VEP assessment blocks. As no significant differences between the two baseline assessments were observed for either component (all *p* values $> .17$), they were averaged in subsequent analyses.

C1 Factor

The C1 factor topography maps showed increased negativity following HFS primarily at Oz (Figure 4A), consistent with the VEP waveforms described earlier. Accordingly, C1 factor scores from Oz were analyzed using a mixed effects model. There was a significant group \times time interaction [$F(3,117) = 6.33, p = .0005$]. Baseline assessments did not significantly differ between groups ($p = .58$). In

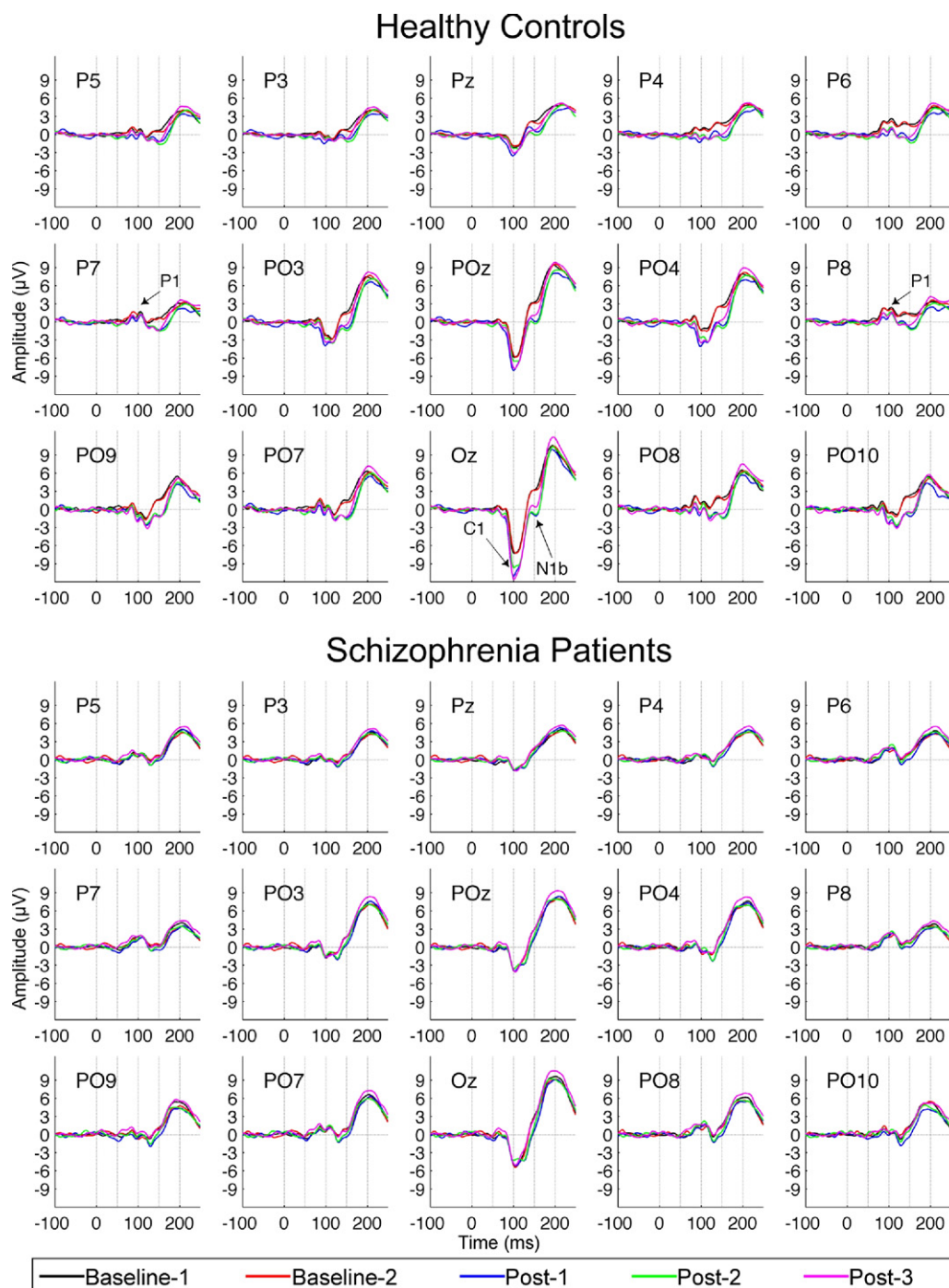


Figure 2. Grand average visual evoked potentials (VEP) elicited by the standard circle are shown for healthy control subjects (HC; $n = 22$; top) and schizophrenia patients (SZ; $n = 19$; bottom) across posterior electrode sites and VEP assessment blocks: Baseline-1 (4–6 minutes before high-frequency stimulation [HFS]; black line), Baseline-2 (2–4 minutes before HFS; red line), Post-1 (2–4 minutes post-HFS; blue line), Post-2 (4–6 minutes post-HFS; green line), and Post-3 (20–22 minutes post-HFS; pink line). The number of trials per VEP assessment block did not differ significantly ($p = .79$) between HC (mean = 76, range = 55–88 trials) and SZ (mean = 75, range = 59–88 trials). In HC, increased negativity of the C1 component (negative peak around 100 msec) is most prominent at the Oz electrode and is evident at all post-HFS VEP assessment blocks. Increased negativity of the N1b component (negative peak around 150 msec) is noticeable in all parietal and parieto-occipital leads, being most prominent at the posterior parieto-occipital leads (P09, P07, Oz, P08, P010) and at all post-HFS assessment blocks. In SZ, the averaged C1 and N1b components do not appear to show any amplitude change over time at any electrode sites. The C1, N1b, and earlier P1 components are indicated by arrows in the HC VEP waveforms (top).

HCS, HFS significantly enhanced C1 negativity at all three post-HFS blocks relative to baseline (all p values $< .002$). In contrast, SZs showed no significant changes in C1 factor scores from baseline to post-HFS assessments (all p values $> .63$). Relative to baseline, C1

factor scores for each post-HFS assessment were significantly more negative in HC than in SZ (all p values $< .02$). The distribution of C1 factor potentiation scores for the two groups is shown in Figure 4C.

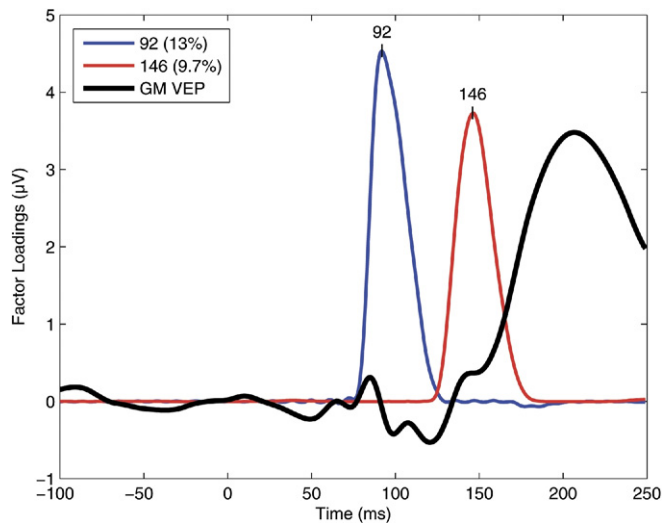


Figure 3. Temporal principal component analysis factor loading waveforms are shown for the two promax-rotated principal component analysis factors whose peak latencies corresponded to the C1 (blue line, peak latency 92 msec) and N1b (red line, peak latency 146 msec) visual evoked potential (VEP) components, respectively. The proportion of the VEP variance accounted for by each component is indicated in the legend box. GM, grand mean.

N1b Factor

The N1b factor topography maps (Figure 5) showed increased negativity following HFS along posterior midline and bilateral parieto-occipital sites in HC, but not in SZ, consistent with the VEP waveforms described above. Accordingly, N1b factor scores were subjected to an off-midline mixed effects analysis of parieto-occipital electrodes grouped by hemisphere (left: P3, P5, P7, PO3, PO7, PO9; right: P4, P6, P8, PO4, PO8, PO10) to test for group, time, and hemisphere effects. A second analysis was conducted on midline electrodes (Pz, POz, Oz). Correlations involving the N1b factor were based on scores averaged over lateral and midline parieto-occipital electrodes.

In the off-midline analysis, there was a significant group × time

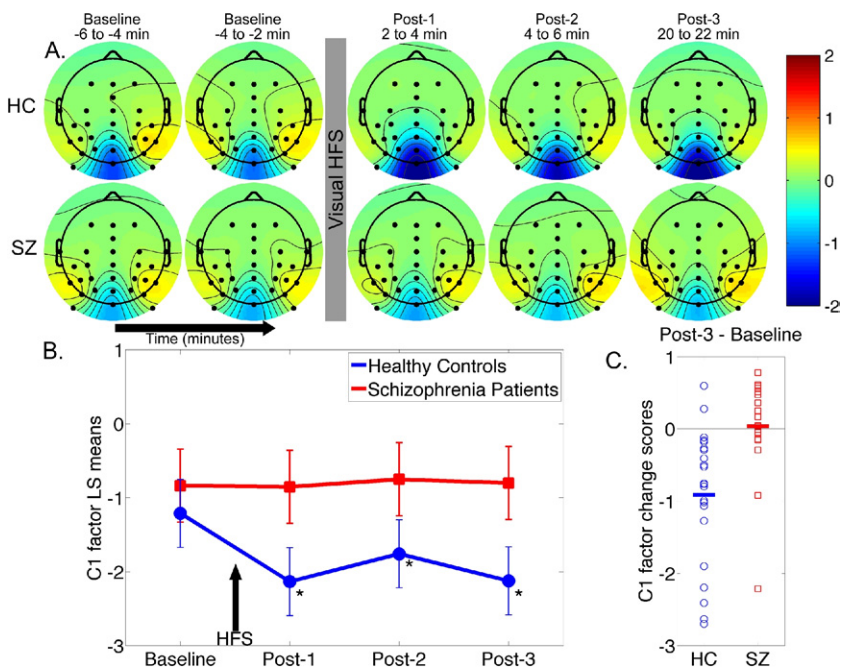


Figure 4. Temporal principal component analysis factor score scalp topography maps are shown for the C1 component. (A) Mean factor score topographies for the C1 component in healthy control subjects (HC) and schizophrenia patients (SZ). Color scale is in standardized units. The prominent negativity at electrode Oz shows sustained potentiation (i.e., increased negativity) following high-frequency stimulation (HFS) in HC but not in SZ. (B) Graph showing the C1 least-squares mean factor scores (± standard error of mean) over time from electrode Oz for HC and SZ. Arrow indicates 2-minute HFS block. (C) Individual subject C1 factor potentiation scores (Post-3 minus Baseline) for HC and SZ (group means are indicated by thick horizontal lines). Baseline, 4 to 6 minutes before HFS and 2 to 4 minutes before HFS; Post-1, 2 to 4 minutes after HFS; Post-2, 4 to 6 minutes after HFS; Post-3, 20 to 22 minutes after HFS.

interaction [$F(3,1470) = 32.24, p < .0001$] that did not significantly interact with hemisphere. Baseline N1b scores did not significantly differ between groups ($p = .69$). In HCs, HFS significantly enhanced N1b negativity at all three post-HFS assessments relative to baseline (all p values $< .0001$). In SZs, HFS significantly enhanced N1b negativity relative to baseline at post-1 and post-2 (p values $< .001$) but not at post-3 ($p = .60$). The change from baseline in N1b was significantly more negative in HC compared with SZ for each post-HFS assessment (all p values $< .0001$). The distribution of N1b factor potentiation scores for the two groups is shown in Figure 5C. The midline electrode analysis yielded essentially the same results, so they are not presented here.

Essentially the same pattern of group × time analysis of variance results were obtained when the C1 and N1b measurements were integrated within fixed windows based on the full-width half maximum values associated with the loading waveforms.

Correlation Between C1 and N1b Potentiation

The relationship between C1 and N1b potentiation at post-3 did not differ between HC and SZ [$F(1,37) = 1.003, p = .32$], nor was the pooled estimate of the common slope significant when the group × N1b potentiation interaction term was dropped from the model [$F(1,38) = .99, p = .33$].

HFS-Driven VSSR and Potentiation of C1 and N1b

Power spectra of EEG recorded during HFS were calculated (shown for electrode Oz in Figures 6A and 6B). The VSSR to HFS is evident in these spectra as a peak power value at ~8.87 Hz, the frequency of the HFS. A summary VSSR power measure was derived by averaging over the parieto-occipital sites where the response was largest (Oz, PO3, POz, PO4, PO7, PO8, PO9, PO10; see Figures 6A and 6B for topography maps).

High-frequency stimulation-driven VSSR power did not differ between HC and SZ [$t(39) = .25, p = .80$; Figure 6]. For regression of C1 and N1b potentiation scores on VSSR and group, the Bonferroni-corrected alpha was set to .025. After ruling out slope differences between groups [$F(1,37) = .31, p = .58$], VSSR power was not significantly related to C1 potentiation [$F(1,38) = 2.90, p = .10$]. In contrast,

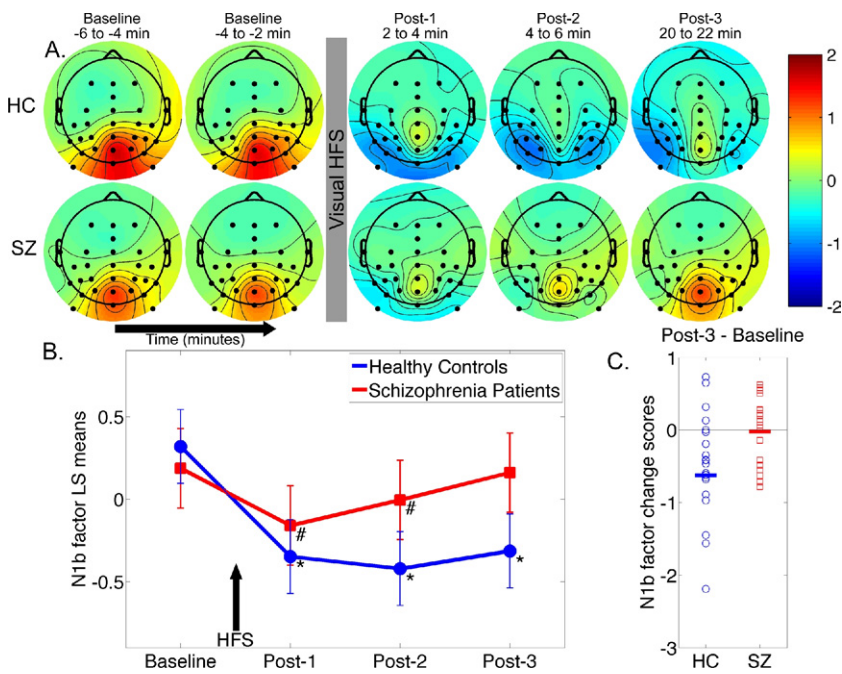


Figure 5. Temporal principal component analysis factor score scalp topography maps are shown for the N1b component. **(A)** Mean factor score topographies for the N1b component in healthy control subjects (HC) and schizophrenia patients (SZ). Color scale is in standardized units. The N1b scores at lateral (P3, P4, P5, P6, P7, P8, PO3, PO4, PO7, PO8, PO9, PO10) and midline (Pz, POz, Oz) parieto-occipital electrodes show sustained potentiation (i.e., increased negativity) following high-frequency stimulation (HFS) in HC. In SZ, potentiation is evident at Post-1 and Post-2 but not at Post-3. **(B)** Graph showing the N1b least-squares mean factor scores (\pm standard error of mean) over time averaged over the lateral parieto-occipital electrodes for HC and SZ. Arrow indicates 2-minute HFS block. **(C)** Individual subject N1b factor potentiation scores (Post-3 minus Baseline) averaged over lateral and midline parieto-occipital electrodes for HC and SZ (group means are indicated with thick horizontal lines). Baseline, 4 to 6 minutes before high-frequency stimulation and 2 to 4 minutes before high-frequency stimulation; Post-1, 2 to 4 minutes after high-frequency stimulation; Post-2, 4 to 6 minutes after high-frequency stimulation; Post-3, 20 to 22 minutes after high-frequency stimulation.

the regression of N1b potentiation on VSSR power showed significant slope differences between the groups [$F(1,37) = 9.38, p = .004$; Figure 6C]. Greater VSSR predicted greater N1b potentiation in HC ($r = -.56, p = .007$) but not SZ ($r = .08, p = .75$).

Changes in Target Reaction Time and Potentiation of C1 and N1b

For regression of C1 and N1b potentiation scores on target reaction time change scores and group, the Bonferroni-corrected alpha was set to .025. For both C1 and N1b potentiation, no significant relationships with reaction time change emerged when slope estimates were pooled across groups. Moreover, the slopes did not significantly differ between the groups. However, within the SZ, greater N1b potentiation significantly correlated with a decrease in target reaction time ($r = .62; p = .005$). This relationship was not evident in the HC ($r = -.086; p = .70$).

Symptom Severity and Potentiation of C1 and N1b

Within SZ, C1 and N1b potentiation scores were not significantly correlated with PANSS Positive or Negative symptom subscales (Bonferroni-corrected alpha = .0125).

Response Accuracy to Oddball Targets

To address whether attentional vigilance throughout VEP baseline and post-HFS assessments was comparable in SZ and HC, visual target response accuracy ("hit rate") was compared in a group \times time nonparametric repeated measures analysis (55). A nonparametric approach was used because there were nontransformable ceiling effects for the hit rates. Neither the main effect of group [analysis of variance type statistic (1) = .02, $p = .88$] nor the group \times time interaction [analysis of variance type statistic (2.84) = 2.10, $p = .10$] was significant.

Discussion

Our results demonstrate that exposure to repetitive visual HFS results in persistent (lasting at least 20 minutes) potentiation of specific visual cortical evoked potentials (C1 at 99 msec and N1b at 147 msec) in HC subjects but not in SZ patients. The potentiated C1

component was largest at Oz, overlaying the primary visual cortex, while the potentiated N1b component was largest at the bilateral occipitoparietal sites, overlaying visual association cortices. In SZ, C1 potentiation was impaired, while enhancement in N1b was short-lasting and returned to baseline by 20 minutes post-HFS.

Clapp *et al.* (11), Teyler *et al.* (14), McNair *et al.* (20), Clapp *et al.* (21), and Ross *et al.* (22) used a similar visual HFS paradigm in healthy subjects to demonstrate that this form of stimulation induces potentiation of the visual N1b. Importantly, this potentiation conformed to the synaptic LTP rules described in animals, including persistence (at least 1 hour), input specificity (only response to the tetanized checkerboard pattern potentiates), frequency-dependency (depression with exposure to low-frequency 1 Hz visual stimulation), and NMDA dependency tested in analogous rat experiments (16). C1 potentiation was not reported (14), likely due to differences in methodology related to visual stimulus presentation (hemi-field vs. full-field) and EEG analysis. Recent reports from another group (17–19), confirm that exposure to visual stimuli in rodents can induce long-lasting potentiation of visual cortical responses, called stimulus-selective response potentiation. This potentiation also has the hallmarks of synaptic LTP, including persistence for days *in vivo*, input specificity, NMDA receptor dependence and insertion of postsynaptic AMPA receptors, mutual occlusion with electrically induced LTP, and protein kinase M ζ activation, known to maintain LTP and memory (17,18). In both cases, the potentiation was expressed at the thalamocortical synapses (16–18). Collectively, these studies indicate that visual stimulation in humans can induce potentiation of visual cortex activation that is measurable with EEG and that shares many characteristics with synaptic LTP.

Several lines of evidence suggested that impairment in visual cortex potentiation in SZs was not due to deficient attention to visual stimuli. First, HCs and SZs showed comparably high hit rates (>90%) to visual oddball targets throughout the task. Second, both HCs and SZs had comparable HFS-driven VSSR EEG power, suggesting that they allocated similar levels of attention and exhibited comparable neuro-oscillatory entrainment to HFS. In animal models, the cellular response (measured as charge transfer) to the elec-

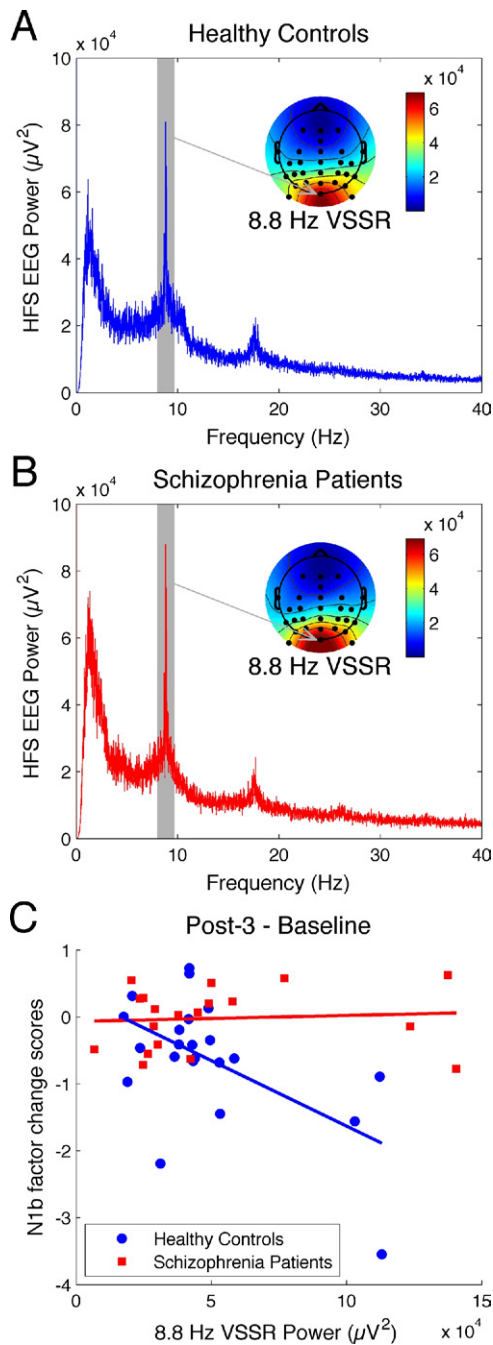


Figure 6. High-frequency stimulation (HFS)-driven visual steady state responses (VSSR) are shown for healthy control subjects (HC) and schizophrenia patients (SZ). **(A)** Grand average electroencephalogram (EEG) power spectrum associated with HFS from electrode Oz in HC (blue line). The VSSR is evident as a peak power value at the HFS driving frequency of ~ 8.8 Hz (gray shading), and the adjacent grand average scalp topography map for the 8.8 Hz VSSR power shows greatest power at Oz and surrounding parieto-occipital electrodes. **(B)** Grand average EEG power spectrum associated with HFS from electrode Oz in SZ (red line), along with grand average scalp topography map for the 8.8 Hz VSSR. The magnitude of the VSSR is comparable in SZ and HC groups. **(C)** N1b component potentiation (Post-3 minus Baseline) is significantly associated with the HFS-driven VSSR power values (averaged over Oz, PO3, POz, PO4, PO7, PO8, PO9, PO10) in HC (blue) but not in SZ (red). Post-3, 20 to 22 minutes after high-frequency stimulation.

trical tetanus is correlated with magnitude of LTP (56,57). Consistent with this, our study provides the first evidence that the magnitude of the EEG VSSR to a visual stimulus presented at high frequency is related to the degree of potentiation of VEP components evoked by that stimulus. In HC, larger HFS-driven VSSR power was correlated significantly with larger N1b potentiation. In contrast, there was no such correlation in SZ subjects, indicating that the mechanism supporting neuronal plasticity, rather than neuronal response to stimuli, was impaired.

Interestingly, in HCs, VSSR correlated significantly with N1b potentiation but not with C1 potentiation, and although both N1b and C1 potentiated, the magnitude of their potentiation did not correlate. These results indicated that the two components are likely expressed by activation of distinct neuronal networks. Indeed, generators of these early visual responses are suggested to be predominantly in the primary (striate) visual cortex for C1 and in the secondary (extrastriate) visual cortex for N1b (58–61). In addition, they are potentially differentially modulated through feedback loops with other brain areas, including the prefrontal cortex (62,63). The negativity in C1 at Oz is likely generated primarily by the thalamocortical input to the principal cells in striate cortex, whereas N1b at the extrastriate cortex is likely a result of the local network activation, including activation of the inhibitory interneurons, driven by input from the striate cortex. As proposed by Clapp *et al.* (11), sensory volleys arriving at the multisynaptic network comprising feedback loops in extrastriate cortex may set off an interneuron-driven synchronization and reverberation, resulting in potentiation of the N1b with different characteristics and modulating factors than the monosynaptic C1 potentiation.

One of the leading hypotheses in schizophrenia posits that NMDA receptor hypofunction may underlie its cognitive and positive symptoms (2,10). Based on this model, hypofunction of NMDA receptors located on the glutamatergic cells would result in impaired LTP, while hypofunction of NMDA receptors located on inhibitory interneurons would result in diminished inhibition. In our work, we find that while C1 potentiation in SZ is completely impaired, there is a short-lasting enhancement in N1b. These results appear to be consistent with the above hypothesis; i.e., while thalamocortical activation of hypofunctioning NMDA receptors on the principal neurons in the primary visual cortex results in impaired C1 potentiation, activation of hypofunctional NMDA receptors located on excitatory as well as inhibitory neurons in association cortices results in transient local disinhibition and short-lasting N1b enhancement.

Induction of sensory potentiation has been associated with enhanced performance in behavioral visual tasks such as visual acuity or discrimination in animals (17) and in humans (11). We did not examine the effect of VEP potentiation on a visual task in this study. However, subjects were asked to respond to a visual target stimulus during the VEP assessments, and their reaction times (speed of processing) were correlated with VEP potentiation. Although SZ patients did not show a significant overall potentiation in N1b when compared with HCs, patients with larger N1b potentiation speeded up their reaction times to the visual target from baseline to the post-3 assessment, indicating that induction of even small and transient potentiation resulted in a behavioral gain. No similar significant association in HCs emerged, possibly because HCs were already performing at their ceiling on this simple task.

This study only examined plasticity impairment in SZ in visual cortex. While this impairment may partially underlie visual processing deficits in SZ (31–40), it is unlikely to account for the entire spectrum of SZ symptomatology. Moreover, while our experiment did not address the competency of neuroplasticity in other cortical

regions, impairment in visual cortex plasticity may reflect more general plasticity dysfunction affecting other cortical regions and sensory modalities, such as the auditory cortex (64). Because the SZ patients in our study were medicated, it is possible that their impaired plasticity was due to antipsychotic medication. This medication confound must be disentangled in future studies.

This study had other limitations, stemming mainly from our motivation to keep the paradigm short for patients. While our design did not include a nontetanized control stimulus to establish that the potentiation observed in HC was specifically due to the visual HFS, previous controlled experiments using similar paradigms have demonstrated that VEP potentiation is specific to the tetanized stimulus (11,14,20,22). In addition, although we only assessed the persistence of VEP potentiation for 20 minutes, prior studies using a similar paradigm (11,14,20,22) have demonstrated persistence of the N1b VEP potentiation for at least 1 hour.

The VEP morphology we observed replicates some studies (14,61,65), but others show earlier C1 onsets (~55 msec) and peaks (~90 msec) (54,66). Moreover, while a P1 component is often prominent following the C1 (54,66), we observed a small bilateral P1 peaking 15 msec earlier than the midline C1 (Figure 2), replicating the Butler *et al.* (65) data. Stimulus and reference site differences may account for this variation.

In summary, our results are consistent with deficient cortical plasticity in SZ. Although this study did not directly examine the role of NMDA receptors, the results and the known mechanism of neuroplasticity in the visual cortex are consistent with the NMDA hypofunction model of SZ. Since many genetic abnormalities associated with SZ risk affect glutamatergic transmission and plasticity (3,4), deficient sensory plasticity may be present before overt symptom onset, potentially providing a predictive biomarker of SZ risk.

This study was funded by National Institutes of Health-National Institute of Mental Health Grant # 1R01 MH06508-01A2 (TT, IC), and by the VA Schizophrenia Biological Research Center (JMF).

Dr. Çavuş is currently employed by Bristol-Myers Squibb, Inc, receives Bristol-Myers Squibb stock options, and reports that her name is included under a provisional patent titled "A noninvasive biomarker of human cortical plasticity and cognition," United States Patent and Trademark Office (USPTO) serial number 61/140,833. Previously she was employed by Pfizer Inc. This work was done during Dr. Çavuş' employment at Yale University. Dr. Teyler reports a consulting appointment with Pfizer Laboratories and that his name is included under a provisional patent titled "A noninvasive biomarker of human cortical plasticity and cognition," USPTO serial number 61/140,833. Dr. Clapp reports that his name is included under a provisional patent titled "A noninvasive biomarker of human cortical plasticity and cognition," USPTO serial number 61/140,833. Dr. Clapp is currently employed full-time as a co-founder and chief scientist at NeuroScouting LLC. This work was done prior to the founding of NeuroScouting, while at Auckland University and University of California San Francisco. Dr. Krystal reports individual consultant agreements (each less than \$10,000 per year) from Aisling Capital, LLC, AstraZeneca Pharmaceuticals, Biocortech, Brintnall & Nicolini, Inc., Easton Associates, Gilead Sciences, Inc., GlaxoSmithKline, Janssen Pharmaceuticals, Lundbeck Research USA, Medivation, Inc., Merz Pharmaceuticals, MK Medical Communications, F. Hoffmann-La Roche Ltd, SK Holdings Co., Ltd, Sunovion Pharmaceuticals, Inc., Takeda Industries, and Teva Pharmaceutical Industries, Ltd. Dr. Krystal also reports serving on the Scientific Advisory Boards for Abbott Laboratories, Bristol-Myers Squibb, Eisai, Inc., Eli Lilly and Co., Forest Laboratories, Inc., Lohocla Research Corporation, Mnesosyne Pharmaceuticals, Inc., Naurex, Inc., Pfizer Pharmaceuticals and Shire Pharmaceuticals. Dr. Krystal also reports Exercisable War-

rant Options from Tetragenex Pharmaceuticals (value less than \$150). Dr. Krystal also reports serving on the Board of Directors of the Coalition for Translational Research in Alcohol and Substance Use Disorders. Dr. Krystal also reports receiving research support from Janssen Research Foundation (provided drug and some study support to the Department of Veterans Affairs). Dr. Krystal also reports serving as Editor of Biological Psychiatry, which is associated with income greater than \$10,000 per year. Dr. Krystal also reports being President for the American College of Neuropsychopharmacology. Dr. Krystal also reports that his name is included on a patent titled "Dopamine and noradrenergic reuptake inhibitors in treatment of schizophrenia" (Patent #:5,447,948, September 5, 1995), and on provisional patents titled "Targeting the glutamatergic system for the treatment of neuropsychiatric disorders" (PCTWO06108055A1) and "Intranasal administration of ketamine to treat depression" (pending). Dr. Mathalon reports research funding from AstraZeneca, Inc, consulting fees from Pfizer, Inc, and that his name is included under a provisional patent titled "A noninvasive biomarker of human cortical plasticity and cognition," USPTO serial number 61/140,833. All other authors report no biomedical financial interests or potential conflicts of interest.

- Goto Y, Yang CR, Otani S (2010): Functional and dysfunctional synaptic plasticity in prefrontal cortex: Roles in psychiatric disorders. *Biol Psychiatry* 67:199–207.
- Stephan KE, Baldeweg T, Friston KJ (2006): Synaptic plasticity and dysfunction in schizophrenia. *Biol Psychiatry* 59:929–939.
- Harrison PJ, Weinberger DR (2005): Schizophrenia genes, gene expression, and neuropathology: On the matter of their convergence. *Mol Psychiatry* 10:40–68; image 5.
- Sebat J, Levy DL, McCarthy SE (2009): Rare structural variants in schizophrenia: One disorder, multiple mutations; one mutation, multiple disorders. *Trends Genet* 25:528–535.
- Kwon OB, Paredes D, Gonzalez CM, Neddens J, Hernandez L, Vullhorst D, Buonanno A (2008): Neuregulin-1 regulates LTP at CA1 hippocampal synapses through activation of dopamine D4 receptors. *Proc Natl Acad Sci U S A* 105:15587–15592.
- Li B, Woo RS, Mei L, Malinow R (2007): The neuregulin-1 receptor erbB4 controls glutamatergic synapse maturation and plasticity. *Neuron* 54:583–597.
- Tang TT, Yang F, Chen BS, Lu Y, Ji Y, Roche KW, Lu B (2009): Dysbindin regulates hippocampal LTP by controlling NMDA receptor surface expression. *Proc Natl Acad Sci U S A* 106:21395–21400.
- Cooke SF, Bliss TV (2006): Plasticity in the human central nervous system. *Brain* 129:1659–1673.
- Stone JM, Erlandsson K, Arstad E, Squassante L, Teneggi V, Bressan RA, *et al.* (2008): Relationship between ketamine-induced psychotic symptoms and NMDA receptor occupancy: a [(123)I]CNS-1261 SPET study. *Psychopharmacology (Berl)* 197:401–408.
- Krystal JH, D'Souza DC, Mathalon D, Perry E, Belger A, Hoffman R (2003): NMDA receptor antagonist effects, cortical glutamatergic function, and schizophrenia: Toward a paradigm shift in medication development. *Psychopharmacology (Berl)* 169:215–233.
- Clapp WC, Hamm JP, Kirk IJ, Teyler TJ (2011): Translating LTP from animals to humans: A novel method for non-invasive assessment of cortical plasticity [published online ahead of print October 3]. *Biol Psychiatry*.
- Daskalakis ZJ, Christensen BK, Fitzgerald PB, Chen R (2008): Dysfunctional neural plasticity in patients with schizophrenia. *Arch Gen Psychiatry* 65:378–385.
- Frantseva MV, Fitzgerald PB, Chen R, Moller B, Daigle M, Daskalakis ZJ (2008): Evidence for impaired long-term potentiation in schizophrenia and its relationship to motor skill learning. *Cereb Cortex* 18:990–996.
- Teyler TJ, Hamm JP, Clapp WC, Johnson BW, Corballis MC, Kirk IJ (2005): Long-term potentiation of human visual evoked responses. *Eur J Neurosci* 21:2045–2050.
- Heynen AJ, Bear MF (2001): Long-term potentiation of thalamocortical transmission in the adult visual cortex in vivo. *J Neurosci* 21:9801–9813.
- Clapp WC, Eckert MJ, Teyler TJ, Abraham WC (2006): Rapid visual stimulation induces N-methyl-D-aspartate receptor-dependent sensory long-term potentiation in the rat cortex. *Neuroreport* 17:511–515.

17. Cooke SF, Bear MF (2010): Visual experience induces long-term potentiation in the primary visual cortex. *J Neurosci* 30:16304–16313.
18. Frenkel MY, Sawtell NB, Diogo AC, Yoon B, Neve RL, Bear MF (2006): Instructive effect of visual experience in mouse visual cortex. *Neuron* 51:339–349.
19. Cooke SF, Bear MF (2012): Stimulus-selective response plasticity in the visual cortex: An assay for the assessment of pathophysiology and treatment of cognitive impairment associated with psychiatric. *Biol Psychiatry* 71:487–495.
20. McNair NA, Clapp WC, Hamm JP, Teyler TJ, Corballis MC, Kirk IJ (2006): Spatial frequency-specific potentiation of human visual-evoked potentials. *Neuroreport* 17:739–741.
21. Clapp WC, Zaehle T, Lutz K, Marcar VL, Kirk IJ, Hamm JP, *et al.* (2005): Effects of long-term potentiation in the human visual cortex: A functional magnetic resonance imaging study. *Neuroreport* 16:1977–1980.
22. Ross RM, McNair NA, Fairhall SL, Clapp WC, Hamm JP, Teyler TJ, Kirk IJ (2008): Induction of orientation-specific LTP-like changes in human visual evoked potentials by rapid sensory stimulation. *Brain Res Bull* 76:97–101.
23. Vialatte FB, Maurice M, Dauwels J, Cichocki A (2010): Steady-state visually evoked potentials: Focus on essential paradigms and future perspectives. *Prog Neurobiol* 90:418–438.
24. Regan MP, Regan D (1989): Objective investigation of visual function using a nondestructive zoom-FFT technique for evoked potential analysis. *Can J Neurol Sci* 16:168–179.
25. Brenner CA, Krishnan GP, Vohs JL, Ahn WY, Hetrick WP, Morzorati SL, O'Donnell BF (2009): Steady state responses: Electrophysiological assessment of sensory function in schizophrenia. *Schizophr Bull* 35:1065–1077.
26. Jin Y, Sandman CA, Wu JC, Bernat J, Potkin SG (1995): Topographic analysis of EEG photic driving in normal and schizophrenic subjects. *Clin Electroencephalogr* 26:102–107.
27. Butler PD, Schechter I, Zemon V, Schwartz SG, Greenstein VC, Gordon J, *et al.* (2001): Dysfunction of early-stage visual processing in schizophrenia. *Am J Psychiatry* 158:1126–1133.
28. Butler PD, Zemon V, Schechter I, Saperstein AM, Hoptman MJ, Lim KO, *et al.* (2005): Early-stage visual processing and cortical amplification deficits in schizophrenia. *Arch Gen Psychiatry* 62:495–504.
29. Ding J, Sperling G, Srinivasan R (2006): Attentional modulation of SSVEP power depends on the network tagged by the flicker frequency. *Cereb Cortex* 16:1016–1029.
30. Clementz BA, Wang J, Keil A (2008): Normal electrocortical facilitation but abnormal target identification during visual sustained attention in schizophrenia. *J Neurosci* 28:13411–13418.
31. Silverstein SM, Bakshi S, Nuernberger S, Carpinello K, Wilkness S (2005): Effects of stimulus structure and target-distracter similarity on the development of visual memory representations in schizophrenia. *Cogn Neuropsychiatry* 10:215–229.
32. Green MF (2006): Cognitive impairment and functional outcome in schizophrenia and bipolar disorder. *J Clin Psychiatry* 67:e12.
33. Nuechterlein KH, Barch DM, Gold JM, Goldberg TE, Green MF, Heaton RK (2004): Identification of separable cognitive factors in schizophrenia. *Schizophr Res* 72:29–39.
34. Skelley SL, Goldberg TE, Egan MF, Weinberger DR, Gold JM (2008): Verbal and visual memory: Characterizing the clinical and intermediate phenotype in schizophrenia. *Schizophr Res* 105:78–85.
35. Butler PD, Javitt DC (2005): Early-stage visual processing deficits in schizophrenia. *Curr Opin Psychiatry* 18:151–157.
36. Butler PD, Silverstein SM, Dakin SC (2008): Visual perception and its impairment in schizophrenia. *Biol Psychiatry* 64:40–47.
37. Green MF, Lee J, Cohen MS, Engel SA, Korb AS, Nuechterlein KH, *et al.* (2009): Functional neuroanatomy of visual masking deficits in schizophrenia. *Arch Gen Psychiatry* 66:1295–1303.
38. Javitt DC (2009): When doors of perception close: Bottom-up models of disrupted cognition in schizophrenia. *Annu Rev Clin Psychol* 5:249–275.
39. Phillips WA, Silverstein SM (2003): Convergence of biological and psychological perspectives on cognitive coordination in schizophrenia. *Behav Brain Sci* 26:65–82; discussion 82–137.
40. Uhlhaas PJ, Phillips WA, Mitchell G, Silverstein SM (2006): Perceptual grouping in disorganized schizophrenia. *Psychiatry Res* 145:105–117.
41. First MB SR, Gibbon M, Williams JBW (1995): *Structured Clinical Interview for DSM-IV Axis I Disorders*. New York: New York State Psychiatric Institute, Biometrics Research Department.
42. Kay SR, Fiszbein A, Opler LA (1987): The Positive and Negative Syndrome Scale (PANSS) for schizophrenia. *Schizophr Bull* 13:261–276.
43. Nurnberger JI Jr, Blehar MC, Kaufmann CA, York-Cooler C, Simpson SG, Harkavy-Friedman J, *et al.* (1994): Diagnostic interview for genetic studies. Rationale, unique features, and training. NIMH Genetics Initiative. *Arch Gen Psychiatry* 51:849–859; discussion 863–864.
44. Crovitz HF, Zener K (1962): A group-test for assessing hand- and eye-dominance. *Am J Psychol* 75:271–276.
45. Hollingshead A (1957): *Hollingshead Two-Factor Index of Social Position*. New Haven, CT: Yale University.
46. Gratton G, Coles MG, Donchin E (1983): A new method for off-line removal of ocular artifact. *Electroencephalogr Clin Neurophysiol* 55:468–484.
47. Kayser J, Tenke CE (2003): Optimizing PCA methodology for ERP component identification and measurement: Theoretical rationale and empirical evaluation. *Clin Neurophysiol* 114:2307–2325.
48. Kayser J, Tenke CE (2005): Trusting in or breaking with convention: Towards a renaissance of principal components analysis in electrophysiology. *Clin Neurophysiol* 116:1747–1753.
49. Dien J, Beal DJ, Berg P (2005): Optimizing principal components analysis of event-related potentials: Matrix type, factor loading weighting, extraction, and rotations. *Clin Neurophysiol* 116:1808–1825.
50. Donchin E (1966): A multivariate approach to the analysis of average evoked potentials. *IEEE Trans Biomed Eng* 13:131–139.
51. Dien J (2010): The ERP PCA Toolkit: An open source program for advanced statistical analysis of event-related potential data. *J Neurosci Methods* 187:138–145.
52. Lyons RG (2004): *Understanding Digital Signal Processing, 2nd ed.* Upper Saddle River, NJ: Prentice Hall PTR.
53. Brown H, Prescott R (1999): *Applied Mixed Models in Medicine*. New York: John Wiley & Sons.
54. Di Russo F, Martinez A, Sereno MI, Pitzalis S, Hillyard SA (2002): Cortical sources of the early components of the visual evoked potential. *Hum Brain Mapp* 15:95–111.
55. Brunner E, Domhof S, Langer F (2002): *Nonparametric Analysis of Longitudinal Data in Factorial Experiments*. New York: Wiley.
56. Aihara T, Tsukada M, Crair MC, Shinomoto S (1997): Stimulus-dependent induction of long-term potentiation in CA1 area of the hippocampus: Experiment and model. *Hippocampus* 7:416–426.
57. Berberich S, Jensen V, Hvalby O, Seeburg PH, Kohr G (2007): The role of NMDAR subtypes and charge transfer during hippocampal LTP induction. *Neuropharmacology* 52:77–86.
58. Pascual-Marqui R, Michel C, Lehmann D (1994): Low resolution electromagnetic tomography: A new method for localizing electrical activity in the brain. *Int J Psychophysiol* 18:49–65.
59. Di Russo F, Martinez A, Sereno M, Pitzalis S, Hillyard SA (2001): Cortical sources of the early components of the visual evoked potential. *Hum Brain Mapp* 15:95–111.
60. Tobimatsu S, Celesia GG (2006): Studies of human visual pathophysiology with visual evoked potentials. *Clin Neurophysiol* 117:1414–1433.
61. Butler SR, Georgiou GA, Glass A, Hancox RJ, Hopper JM, Smith KR (1987): Cortical generators of the CI component of the pattern-onset visual evoked potential. *Electroencephalogr Clin Neurophysiol* 68:256–267.
62. Foxe JJ, Simpson GV (2002): Flow of activation from V1 to frontal cortex in humans. A framework for defining “early” visual processing. *Exp Brain Res* 142:139–150.
63. Barcelo F, Suwazono S, Knight RT (2000): Prefrontal modulation of visual processing in humans. *Nat Neurosci* 3:399–403.
64. Mears RP, Spencer KM (2012): Electrophysiological assessment of auditory stimulus-specific plasticity in schizophrenia. *Biol Psychiatry* 71:503–511.
65. Butler PD, Martinez A, Foxe JJ, Kim D, Zemon V, Silipo G, *et al.* (2007): Subcortical visual dysfunction in schizophrenia drives secondary cortical impairments. *Brain* 130:417–430.
66. Fu S, Fedota JR, Greenwood PM, Parasuraman R (2010): Dissociation of visual C1 and P1 components as a function of attentional load: An event-related potential study. *Biol Psychol* 85:171–178.